nature cell biology

GEP100 links epidermal growth factor receptor signalling to Arf6 activation to induce breast cancer invasion

Masaki Morishige[1,2,9], Shigeru Hashimoto[1,9], Eiji Ogawa[3,4], Yoshinobu Toda[5], Hirokazu Kotani[4,5], Mayumi Hirose[6], Shumei Wei[1], Ari Hashimoto[1], Atsuko Yamada[1], Hajime Yano[1], Yuichi Mazaki[1], Hiroshi Kodama[7], Yoshinori Nio[7], Toshiaki Manabe[4], Hiromi Wada[3], Hidenori Kobayashi[2] and Hisataka Sabe[1,8,10]

Epidermal growth factor (EGF) receptor (EGFR) signalling is implicated in tumour invasion and metastasis[1,2]. However, whether there are EGFR signalling pathways specifically used for tumour invasion still remains elusive. Overexpression of Arf6 and its effector, AMAP1, correlates with and is crucial for the invasive phenotypes of different breast cancer cells[3–6]. Here we identify the mechanism by which Arf6 is activated to induce tumour invasion. We found that GEP100/BRAG2, a guanine nucleotide exchanging factor (GEF) for Arf6, is responsible for the invasive activity of MDA-MB-231 breast cancer cells, whereas the other ArfGEFs are not. GEP100, through its pleckstrin homology domain, bound directly to Tyr1068/1086-phosphorylated EGFR to activate Arf6. Overexpression of GEP100, together with Arf6, caused non-invasive MCF7 cells[7] to become invasive, which was dependent on EGF stimulation. Moreover, GEP100 knockdown blocked tumour metastasis. GEP100 was expressed in 70% of primary breast ductal carcinomas, and was preferentially co-expressed with EGFR in the malignant cases. Our results indicate that GEP100 links EGFR signalling to Arf6 activation to induce invasive activities of some breast cancer cells, and hence may contribute to their metastasis and malignancy.

Invasive and metastatic abilities are fundamental components of tumour malignancy. Tumour malignancy often correlates with proliferative phenotypes, such as expression or overexpression of EGFR/ErbB1, ErbB2/Neu/Her2 and hepatocyte growth factor (HGF) receptor/c-Met, in different types of tumour including primary breast tumours[1,2,8]. Many reports have described signalling pathways downstream of these receptors that participate in the invasive activities[1,2,8]. For the development of tumour therapeutics, however, it is important to identify signalling pathways that are specifically used in tumour invasion, but rarely used in normal cells. It is also important to identify which signalling pathways are central to tumour invasion.

We have shown that Arf6, a small GTPase, is overexpressed in highly invasive breast cancer cells and plays an essential role during invasion, whereas Arf6 expression is marginal in weakly and non-invasive breast cancer cells, and in normal mammary epithelial cells[3,5]. We have subsequently identified that AMAP1 acts as an effector for GTP-Arf6 to induce invasive activities[4,6]. AMAP1 is also overexpressed in highly invasive breast cancer cells, and blocking AMAP1 function inhibits their invasion and metastasis[4,6,9]. AMAP1 expression, moreover, correlates well with the invasive phenotypes and malignancy of primary breast tumours[4]. Therefore, Arf6 and AMAP1 appear to constitute a signalling axis, specifically involved in and central to the invasion and metastasis of some breast tumours, but not generally used in normal mammary epithelia.

More than a single type of GEF activates Arf6 (refs 10, 11). Here we identify an ArfGEF responsible for tumour invasion, and show the mechanism by which Arf6 is activated to induce tumour invasion. The pathway described in this report appears to be used in a significant population of primary breast tumours, and contributes to their malignancy.

There are 15 genes in humans encoding proteins bearing the *Sec7* domain, a putative ArfGEF domain[10,11]. Using the highly invasive breast-cancer cell line MDA-MB-231 as a model, we first examined which ArfGEFs are expressed in this cell line. MDA-MB-231 cells expressed 10 different ArfGEF messenger RNA (mRNAs; Fig. 1a), and their proteins (Fig. 1b). In this analysis we excluded Fbx8, because this protein is an E3 ligase for Arf6 (to be published elsewhere). Among these 10 ArfGEFs, small

[1]Department of Molecular Biology, Osaka Bioscience Institute, Osaka 565-0874, Japan. [2]Department of Neurosurgery, School of Medicine, Oita University, Oita 879-5593, Japan. [3]Department of Thoracic Surgery, Faculty of Medicine, Kyoto University, Kyoto 606-8507, Japan. [4]Laboratory of Diagnostic Pathology, Kyoto University Hospital, Kyoto 606-8501, Japan. [5]Center for Anatomical Studies, Kyoto University Graduate School of Medicine, Kyoto 606-8507, Japan. [6]Laboratory of Supramolecular Crystallography, Institute for Protein Research, Osaka University, Osaka 565-0871, Japan. [7]Kodama Breast Clinic, Kyoto 603-8325, Japan. [8]Graduate School of Biosciences, Kyoto University, Kyoto 606-8607, Japan.
[9]These authors contributed equally to this work.
[10]Correspondence should be addressed to H.S. (sabe@obi.or.jp)

Received 31 July 2007; accepted 21 November 2007, published online 16 December 2007; DOI: 10.1038/ncb1672

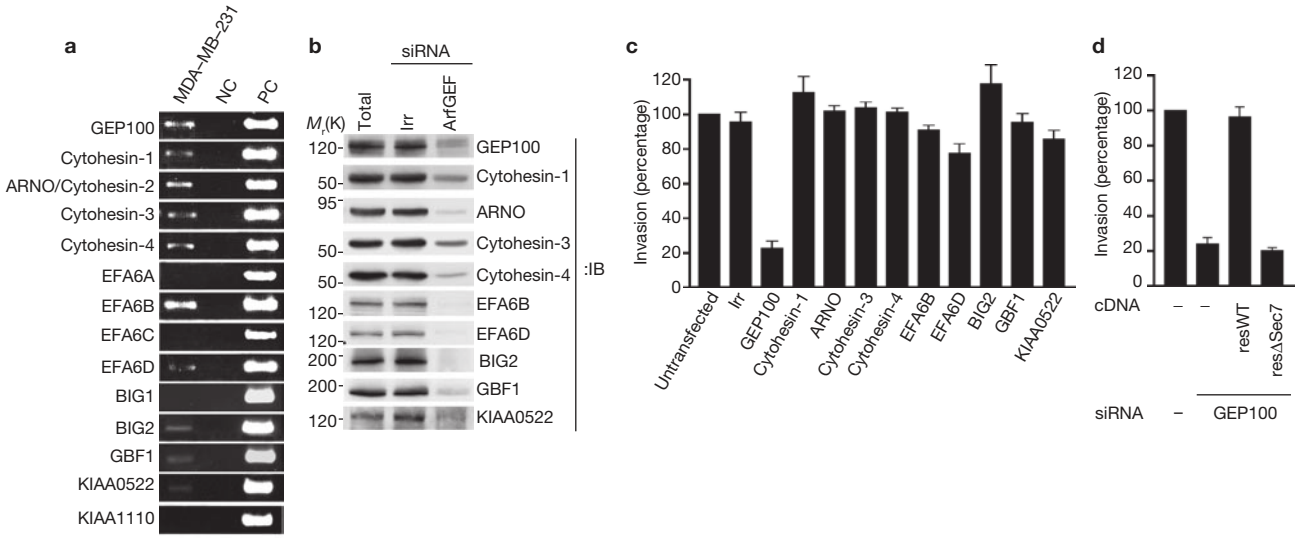

Figure 1 GEP100 is responsible for the Matrigel invasion activity of MDA-MB-231 cells. (**a**) Expression of ArfGEF mRNAs was analysed by using RT–PCR, coupled with agarose gel electrophoresis. cDNA (2 ng) corresponding to each indicated ArfGEF was used as positive control (PC). NC, without template cDNAs. (**b**, **c**) Cells, untransfected or transfected with siRNA duplexes against each indicated ArfGEF, or with irrelevant sequences (Irr), were analysed for their expression of ArfGEFs by immunoblotting of the lysates by using each corresponding ArfGEF antibody, as indicated (**b**); or were subjected to the Matrigel invasion assay using NIH3T3 conditioned media as chemoattractants (**c**). Blots of cell lysates (10 μg), without siRNA treatment, are also shown (Total, **b**). (**d**) Cells treated with a GEP100 siRNA were transfected with a rescue construct of wild-type GEP100 cDNA (resWT) or its Sec7-deletion mutant (resΔSec7), and analysed for their Matrigel invasion activities as in **c**. Untreated cells are also included as a control (left column). In **c** and **d**, data are presented as percentages calculated by normalizing the values obtained for the untreated cells as 100%. Error bars show mean ± s.e.m., $n = 3$. Untreated cells (3597 ± 415, that is, about 3.6% of the initially loaded cells) were calculated to have transmigrated per ϕ6.4 mm Matrigel-coated Boyden chamber filter under these conditions (see also Methods). Uncropped images of blots are shown in Supplementary Fig. 6.

interfering RNA (siRNA)-mediated knockdown of GEP100 significantly blocked the Matrigel invasion activity (Fig. 1b, c). GEP100 is a specific GEF for Arf6 (ref. 12). On the other hand, knockdown of none of the other ArfGEFs, including ARNO/Cytohesin-2 (ref. 13) and EFA6B[14] (both are also robust GEFs for Arf6), blocked the invasion (Fig. 1b, c). The viability, adhesion and haptotactic migration were almost unaffected by GEP100 siRNA treatment (Supplementary Fig. 1a–c). Moreover, a Sec7 domain-deleted mutant (ΔSec7) of the GEP100 rescue construct did not restore the invasion activity in GEP100 siRNA-treated cells, whereas the wild-type construct did (Fig. 1d). To assess more precisely whether invasiveness of a substantial population of tumour cells is blocked by GEP100 knockdown (see Methods), we also examined its effects on invadopodia formation. GEP100 knockdown robustly inhibited invadopodia formation of MDA-MB-231 cells, in which about 70% of the untreated cells formed significantly large invadopodia (Supplementary Fig. 1d). These results suggest that GEP100, but not other ArfGEFs, is specifically responsible for the invasive activities of MDA-MB-231 cells. Knockdown of Arf6 does not affect the secretion of active MMP2 and MMP9 (ref. 3). Similarly, knockdown of GEP100 did not affect their secretion (see Supplementary Fig. 1e).

The above Matrigel invasion assay was performed by using conditioned medium prepared from NIH3T3 cells as a source of chemoattractants[3,4]. MDA-MB-231 cells express EGFR and respond to EGF to be invasive[15]. Moreover, EGF stimulation has been implicated in Arf6 activation[16]. We then examined whether GEP100, as well as Arf6, are located downstream of EGFR in the induction of invasive activities. Knockdown of Arf6 and GEP100 each effectively blocked the EGF-induced Matrigel invasion (Fig. 2a). Moreover, activities of endogenous Arf6, measured by using the glutathione *S*-transferase (GST)–golgi-localized, γ-ear-containing, Arf-binding protein (GGA) pulldown method[13], were clearly enhanced upon EGF stimulation, and this enhancement was substantially abolished by GEP100 knockdown (Fig. 2b).

We then found that endogenous GEP100 is co-precipitated with endogenous EGFR in MDA-MB-231 cells upon EGF stimulation (Fig. 2c). MDA-MB-231 cells express ErbB2 at a moderate level[17], which is an EGFR-family member and able to form a heterodimer with EGFR[2]. ErbB2 was not detected in these anti-GEP100 immunoprecipitants (Fig. 2c). We then expressed enhanced green fluorescent protein (EGFP)-tagged EGFR and myc-tagged GEP100 in Cos-7 cells, and confirmed the co-precipitation of myc-GEP100 with EGFR-EGFP upon EGF stimulation also in this reconstituted system (Fig. 2d). We also confirmed Arf6 activation by GEP100 and ligand-activated EGFR in the reconstituted system, by expressing haemagglutinin-tagged Arf (Arf6–HA), myc-GEP100 and EGFR-EGFP in Cos-7 cells (Fig. 2e). The Sec7 domain of GEP100 was indispensable for this Arf6 activation (Fig. 2e). On the other hand, expression of myc-ARNO or myc-EFA6B induced constitutive activation of Arf6 regardless of EGF stimulation (Fig. 2e). Expression of myc-BIG2 (ref. 18), a GEF for Arf1-3, did not enhance Arf6 activity (Fig. 2e). These results collectively indicate that GEP100 specifically associates with EGFR to activate Arf6, upon EGF stimulation.

We next investigated the mechanism by which GEP100 associates with the ligand-activated EGFR. GEP100 does not bear any apparent protein binding modules, known to bind to activated EGFR. We made a series of GEP100 mutants and found that deletion of the pleckstrin homology domain (ΔPH), but not its amino (N)-terminal (ΔN) or Sec7 (ΔSec7) domains, abolishes association of GEP100 with ligand-activated EGFR (Fig. 2d). Moreover, this PH domain alone, fused to GST, bound

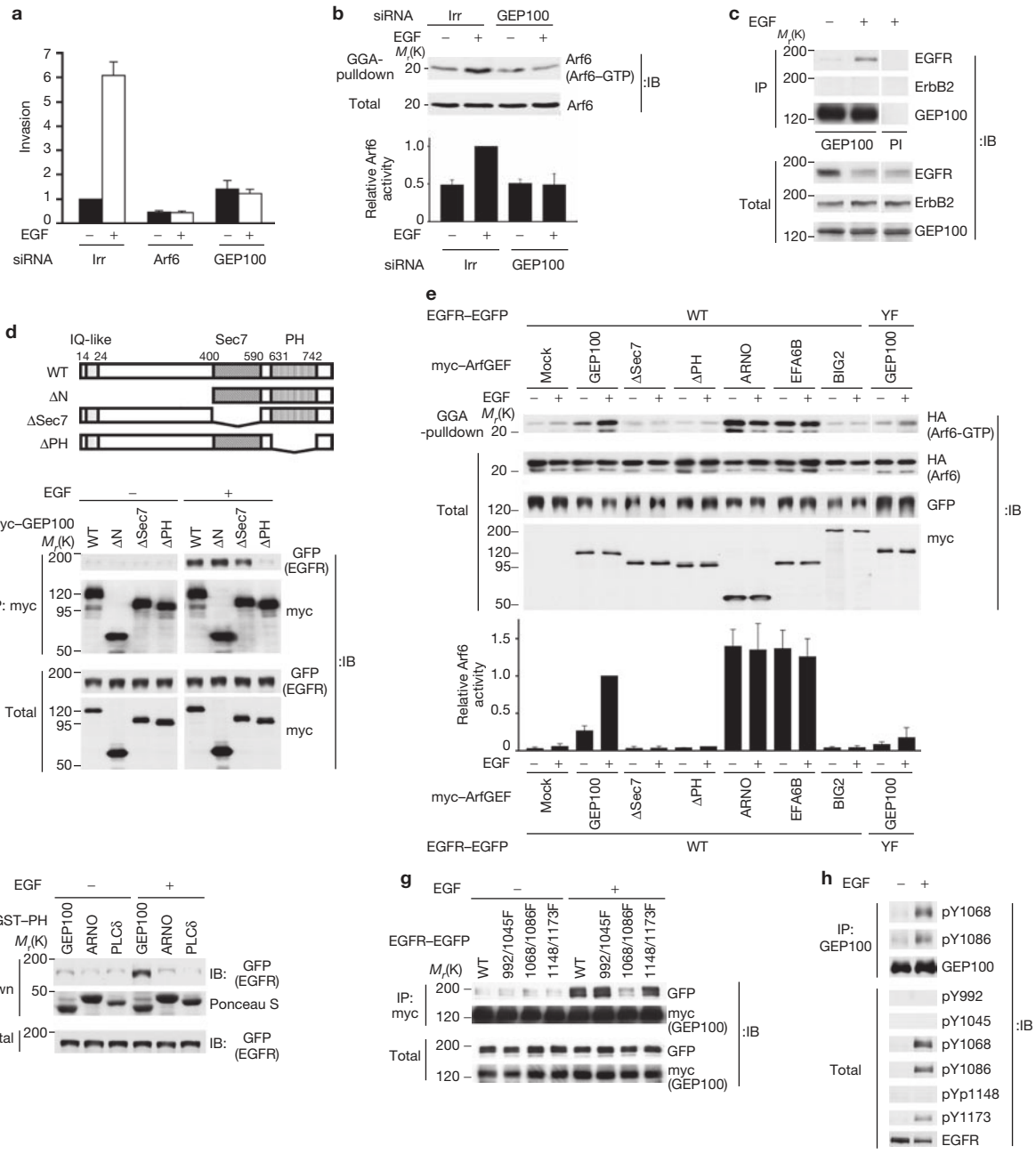

Figure 2 GEP100 associates with ligand-activated EGFR to induce Arf6 activation and tumour invasion. (**a**, **b**) Matrigel invasion activities (**a**) and Arf6 activities (**b**) of MDA-MB-231 cells, transfected with siRNAs for Arf6, GEP100 or irrelevant sequences (Irr), in the presence or absence of EGF (10 ng ml^{-1}). In **a**, the vertical axis indicates the fold increase of activities compared with those of the control cells without EGF. Control cells (824 ± 92 and 4944 ± 299) in the absence and presence of EGF, respectively (that is, about 0.8% and 4.9% of the initially loaded cells, respectively) had transmigrated. (**c**) Co-precipitation of GEP100 with EGFR in MDA-MB-231 cells, analysed by anti-GEP100 immunoprecipitation (IP) and anti-EGFR immunoblot. Anti-ErbB2 immunoblot was also included. PI, pre-immune serum. About 2% of EGFR was co-precipitated with GEP100 upon EGF stimulation. (**d**) Co-precipitation of EGFR-EGFP with myc-GEP100 or its mutants (ΔN, ΔSec7 and ΔPH), analysed by anti-myc immunoprecipitation and anti-GFP immunoblots. (**e**) Arf6-HA activities in cells expressing EGFR-EGFP and myc-GEP100 or their mutants, measured by GST-GGA pulldown and anti-HA immunoblots. WT, wild-type EGFR-EGFP; YF, the 1068/1086F mutant. Mock: transfection with EGFR-EGFP and Arf6-HA, but not myc-ArfGEFs. (**f**) *In vitro* co-precipitation of EGFR-EGFP with indicated GST-fused pleckstrin homology domains, analysed by glutathione-beads pulldown and anti-GFP immunoblots. GST-fusion proteins were visualized by Ponceau S. (**g**) Co-precipitation of myc-GEP100 with wild-type EGFR-EGFP (WT) or its mutants (992/1045F, 1068/1086F and 1148/1173F), analysed by anti-myc immunoprecipitation and anti-GFP immunoblots. (**h**) Phosphorylation of Tyr1068 (pY1068) and Tyr1086 (pY1086) of EGFR and its co-precipitation with GEP100 in MDA-MB-231 cells, analysed by using phosphotyrosine-specific antibodies and anti-GEP100 immunoprecipitation. These assays were performed at least twice and a representative figure is shown. Error bars show mean ± s.e.m., $n = 3$. Total, total cell lysates (10 μg). Relative values are shown by normalizing the value obtained for the EGF- and irrelevant siRNA-treated cells to 1.0 (**b**); and the value obtained for the EGF-treated cells, expressing EGFR-EGFP and myc-GEP100, to 1.0 (**e**) (lower panels). In **b**–**h**, EGF (10 ng ml^{-1}) treatments were for 10 min. Uncropped images of blots are shown in Supplementary Fig. 6.

TABLE 1 Summary of immunohistochemical analysis of surgical specimens of human breast cancer.

DCIS				
Total	**GEP100 positive**	**EGFR positive**	**GEP100/EGFR double-positive**	**GEP100/EGFR double-negative**
72	45 (62.5%)	29 (40.3%)	24 (33.3%)	22 (30.6%)
Grade (*n*)				
1 (21)	11 (52.4%)	7 (33.3%)	4 (19.1%)	7 (33.3%)
2 (29)	20 (69.0%)	13 (44.8%)	11 (37.9%)	7 (24.1%)
3 (22)	14 (63.6%)	9 (40.9%)	9 (40.9%)	8 (36.4%)
IDC				
Total	**GEP100 positive**	**EGFR positive**	**GEP100/EGFR double-positive**	**GEP100/EGFR double-negative**
30	25 (83.3%)	12 (40.0%)	11 (36.7%)	4 (13.3%)
ILC				
Total	**GEP100 positive**	**EGFR positive**	**GEP100/EGFR double-positive**	**GEP100/EGFR double-negative**
12	4 (33.3%)	3 (25.0%)	2 (16.7%)	7 (58.3%)

The expression patterns of GEP100 and EGFR in 72 samples of DCIS, 30 samples of IDC and 12 samples of ILC were determined and summarized

to ligand-activated EGFR *in vitro*, whereas PH domains from ARNO and phospholipase Cδ (PLCδ)[19] did not (Fig. 2f). EGFR has six major tyrosine phosphorylation sites, induced upon EGF stimulation[2]. We found that simultaneous mutation of both Tyr1068 and Tyr1086 into phenylalanines (1068/1086F) abolishes the association of EGFR with GEP100 in Cos7 cells, whereas their single mutation does not (Fig. 2g, and data not shown). Mutations of other tyrosines (Tyr992, 1045, 1148 and 1173) into phenylalanines, singly or in combinations, did not abolish their association (Fig. 2g, 992/1045F, 1148/1173F; data not shown). The 1068/1086F mutant of EGFR-EGFP did not cause activation of Arf6-HA, in Cos-7 cells expressing myc-GEP100 and stimulated by EGF (Fig. 2e, YF). Although most PH domains exhibit some affinity to phosphoinositides, only about 15% of them bind specifically to phosphoinositides, and the physiological role of most of the remaining PH domains has not been clarified[20]. Tyr1068 and Tyr1086 have a common motif of Tyr-X-Asn-Gln[2]. We tested whether the GEP100 PH domain binds directly to phosphorylated Tyr1068- and Tyr1086-peptides, by blotting these peptides onto membrane filters followed by incubation with the GST–GEP100 PH protein. GST–GEP100 PH bound almost equally to phosphorylated Tyr1068- and Tyr1086 peptides, but not to their non-phosphorylated forms (see Supplementary Fig. 2). The simultaneous presence of these two phosphorylated peptides did not show enhanced binding to GST–GEP100 PH (see Supplementary Fig. 2). On the other hand, GST–GEP100 PH did not bind to Tyr992-, Tyr1045-, Tyr1148- and Tyr1173-peptides, regardless of their phosphorylation (see Supplementary Fig. 2). Moreover, the ARNO PH domain did not bind to phosphorylated Tyr1068- and Tyr1086-peptides (see Supplementary Fig. 2). EGFR became phosphorylated at Tyr1068 (pY1068) and Tyr1086 (pY1086) in MDA-MB-231 cells upon EGF stimulation; and Tyr1068- and Tyr1086-phosphorylated EGFR was co-immunoprecipitated with GEP100 upon EGF stimulation (Fig. 2h). Taken together, these results indicate that the GEP100 and EGFR complex, formed upon ligand-activation of EGFR, is mediated by their direct interaction, most likely through the binding of the GEP100 PH domain either to the Tyr1068- or Tyr1086-phosphorylation sites of EGFR.

Invasive characters are diverse even among the different cell lines of breast carcinomas[21,22]. We then sought to obtain evidence supporting the involvement of GEP100 in the invasive activities of various different breast cancer cells. Hs578T and MDA-MB-435s cells also use Arf6 activities for their invasion[3]. Knockdown of GEP100 also significantly inhibited their Matrigel invasion activities (see Supplementary Fig. 3a). We then performed immunohistochemical analyses. About 60% of the ductal carcinoma *in situ* specimens (DCIS, *n*=72) were positive for GEP100, whereas about 40% of them were positive for EGFR (Table 1, and Supplementary Fig. 3b). Notably, although expression of GEP100 *per se* or EGFR *per se* did not correlate with the tumour grade, their co-expression increased in grade 2 and grade 3 tumours compared with grade 1 tumours (Table 1). Moreover, more than 90% of EGFR-positive grade 2 and 3 tumours were positive for GEP100 ((11 + 9)/(13 + 9) cases; Table 1), whereas about 57% of EGFR-positive grade 1 tumours were positive for GEP100 (4/7 cases, Table 1). This increase in GEP100-positive tumours among the EGFR-positive tumours in grade 2/3 versus grade 1 is statistically significant (P=0.0394). On the other hand, more than 80% of invasive ductal carcinoma specimens (IDC; *n*=30) were positive for GEP100, and about 37% of them were double positive for GEP100 and EGFR (Table 1 and Supplementary Information, Fig. S3b). The increase in GEP100-positive tumours in IDC versus DCIS (including grades 1, 2 and 3) is also statistically significant (P=0.0388). As in the case of the DCIS grade2/3 specimens, more than 90% of these IDC specimens, which were positive for EGFR, were also positive for GEP100 (11/12 cases, Table 1). We also examined invasive lobular carcinoma (ILC, *n*=12). Four of these samples were positive for GEP100, and three were positive for EGFR (Table 1, and Supplementary Fig. 3b). Among the three samples positive for EGFR, two were also positive for GEP100.

We next investigated whether forced expression of GEP100 can give rise to invasiveness in non-invasive breast cancer cells, such as MCF7 cells[7]. MCF7 cells express low levels of Arf6 (ref. 3) and GEP100 (Supplementary Fig. 4a). On the other hand, they express EGFR and respond well to EGF to proliferate[23]. We found that

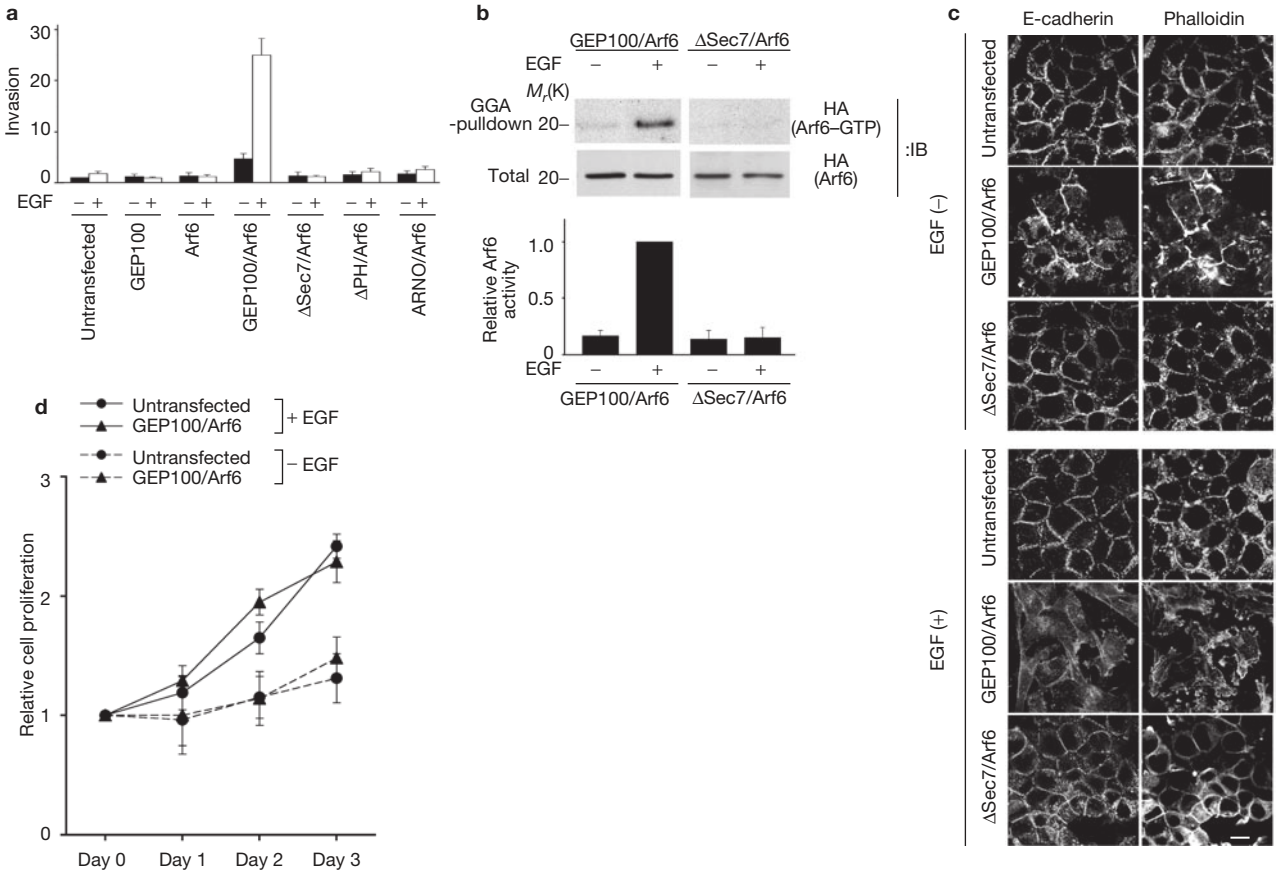

Figure 3 Co-expression of GEP100 and Arf6 evokes EGF-dependent invasiveness in MCF7 cells. Untransfected cells, or cells transfected with pIRES plasmids encoding EGFP-GEP100 alone, EGFP/IRES/Arf6-HA, EGFP-GEP100/IRES/Arf6-HA, EGFP-GEP100(ΔSec7)/IRES/Arf6-HA, EGFP-GEP100(ΔPH)/IRES/Arf6-HA or EGFP-ARNO/IRES/Arf6-HA (untransfected, GEP100, Arf6, GEP100/Arf6, ΔSec7/Arf6, ΔPH/Arf6 and ARNO/Arf6, respectively); and EGFP-bright positive cells were sorted before analyses. (**a**, **b**) Matrigel invasion activities (**a**) and Arf6-HA activities (**b**) were measured in the presence or absence of EGF (10 ng ml^{-1}). In **a**, numbers indicate the fold increase of invasion compared with untransfected cells without EGF stimulation. Error bars show mean ± s.e.m., $n = 3$. Untransfected cells (119 ± 28, that is, about 0.1% of the initially loaded cells) were calculated to have transmigrated per ϕ6.4 mm filter in the absence of EGF, whereas 3511 ± 433 of the GEP100/Arf6 cells (that is, about 3.5% of the initially loaded cells) had transmigrated in the presence of EGF. In **b**, cells were either untreated or treated with 10 ng ml^{-1} EGF for 10 min before subjecting to analyses, as indicated. GGA-pulldown assays were performed three times and a representative figure is shown. Total includes 10 μg of total cell lysates. Relative values are shown by normalizing the value obtained for the EGF-treated cells, expressing myc-GEP100 and Arf6-HA, to 1.0 (lower panel). Error bars show mean ± s.e.m., $n = 3$. (**c**) E-cadherin-mediated cell–cell adhesions. Sorted cells, as indicated, were starved for 20 h, then cultured in the presence or absence of EGF (10 ng ml^{-1}) for 12 h, and labelled with an anti-E-cadherin antibody coupled with Cy3-conjugated anti-mouse IgG, and Alexa Fluor 647-labelled phalloidin as indicated. More than 100 cells were observed in each of three independent experiments, and representative images are shown. Scale bar, 20 μm. (**d**) Proliferation of cells, as indicated, was measured in the presence or absence of EGF (10 ng ml^{-1}) for three days. Error bars show mean ± s.e.m., $n = 3$. Uncropped images of blots are shown in Supplementary Fig. 6.

although overexpression of either EGFP-tagged GEP100 or Arf6-HA alone does not induce notable Matrigel invasion activity in MCF7 cells, simultaneous overexpression of EGFP-GEP100 and Arf6-HA induces appreciable invasion activity, dependent on EGF stimulation (Fig. 3a). Both the Sec7 and PH domains of GEP100 were required for this activity (Fig. 3a). On the other hand, expression of EGFP-ARNO, together with Arf6-HA, did not cause MCF7 cells to become notably invasive (Fig. 3a). EGF-dependent activation of Arf6-HA in MCF7 cells was detected by expression of EGFP-GEP100, but not by the ΔSec7 mutant (Fig. 3b). Formation of E-cadherin-mediated cell–cell adhesion is one of the major properties that maintain the non-invasive phenotypes of various carcinomas[24,25]. Formation of E-cadherin-mediated cell–cell adhesion, seen in the intact MCF7 cells, was substantially impaired in the presence of EGF by co-overexpression of EGFP-GEP100 and Arf6-HA, but not by the ΔSec7 mutant and Arf6-HA, or EGFP alone (Fig. 3c, and data not shown). Co-overexpression of EGFP-GEP100 and Arf6-HA did not affect the proliferation of MCF7 cells (Fig. 3d). These results, taken together, further support the possible use of the EGFR/GEP100/Arf6 pathway in different breast cancer cells, and the specific role of this pathway in the acquisition of invasive phenotypes. Moreover, signalling through GEP100 and Arf6 appears to have the potential to perturb E-cadherin functions at cell–cell contacts, although we have yet to analyse its precise mechanism. We confirmed comparable levels of expression of EGFP-GEP100, Arf6-HA and endogenous E-cadherin in these cells (Supplementary Fig. 4b).

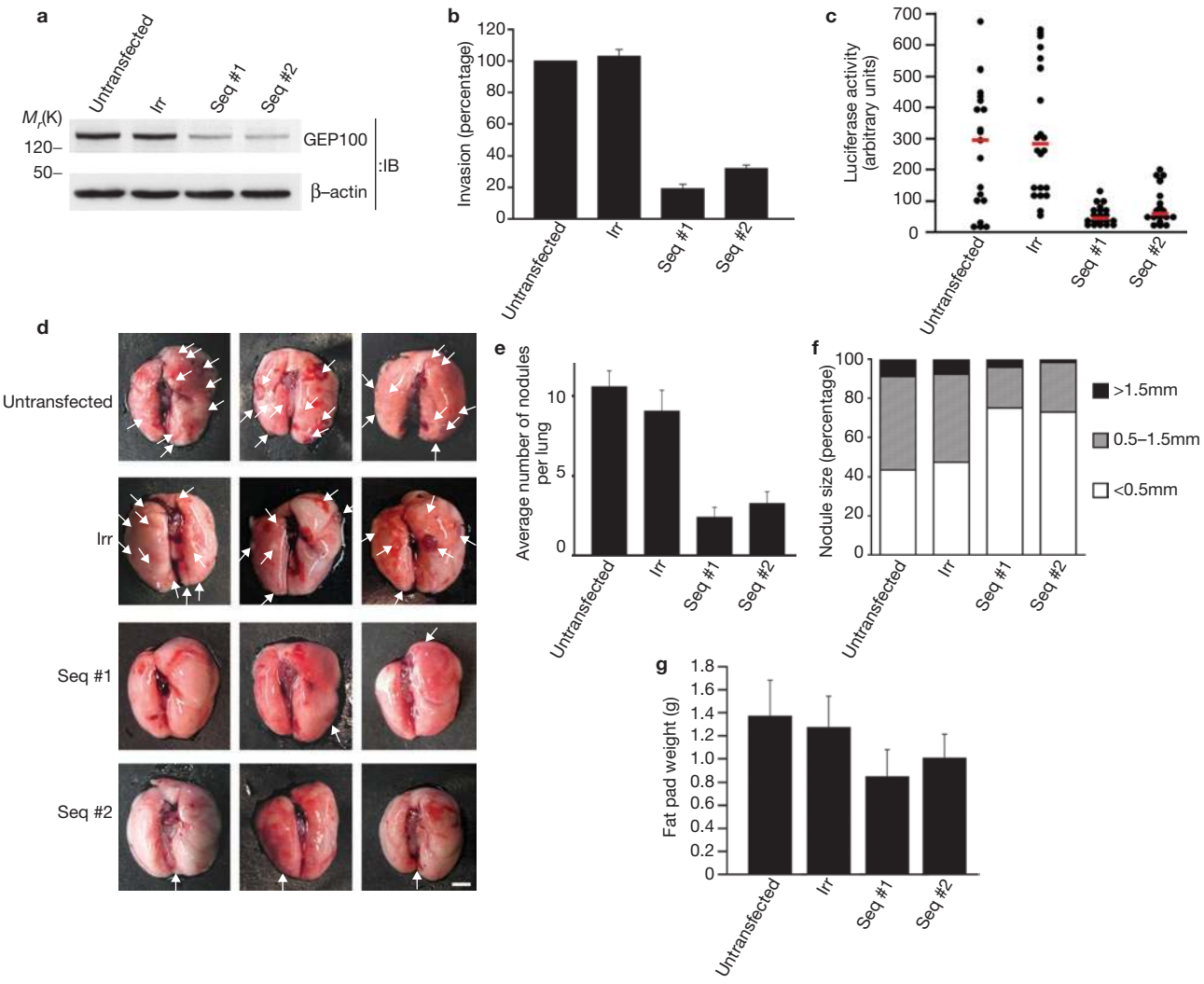

Figure 4 Silencing of GEP100 blocks lung metastasis in mice. 4T1/luc cells, untransfected or transfected with plasmids encoding GEP100 shRNA sequences (Seq #1 and Seq #2) or an irrelevant sequence (Irr), were analysed for their GEP100 expression (**a**), Matrigel invasion (**b**) and lung metastasis (**c**–**f**). Tumour growth at the originally injected sites was also measured in metastasis assays (**g**). In **a**, a β-actin immunoblot was included as a control. In **b**, data are presented as percentages calculated by normalizing the values obtained for the untreated cells as 100%, in which 2958 ± 192 cells (that is, about 3.0% of the initially loaded cells) were calculated to have transmigrated per ϕ6.4 mm filter. In **c**, median values are shown as red lines. In **d**–**f**, photographs representing lung metastases (arrows indicate metastatic nodules (**d**)), average numbers of metastatic nodules (**e**) and apparent sizes of each metastatic nodule (**f**) on the surface of each lung are shown. Error bars show mean ± s.e.m., $n = 3$, 19 and 20 for **b**, **e** and **g**, respectively. Uncropped images of blots are shown in Supplementary Fig. 6.

Finally, we examined whether knockdown of GEP100 blocks tumour metastasis *in vivo*. Arf6 and AMAP1 are also essential for invasion and metastasis of mouse mammary-tumour cell-line 4T1/luc[4,9]. We generated two sets of plasmids, each encoding different **short hairpin RNA** (shRNA) specific to mouse *GEP100* mRNA. Each plasmid efficiently blocked GEP100 expression and Matrigel invasion activity of 4T1/luc cells (Fig. 4a, b). We then measured the lung metastasis of these 4T1/luc cells, by injecting them into the mammary fat pads of Balb/c mice, syngenic to 4T1/luc cells. Metastatic activities of 4T1/luc cells, assessed by their luciferase activities, were also severely suppressed by these GEP100 shRNAs compared with that by the control shRNA, whereas tumour growth at the original sites of injection was only slightly inhibited by these GEP100 shRNAs (Fig. 4c, g). The numbers as well as the sizes of metastatic nodules on the surface of the lungs were also reduced by GEP100 shRNAs (Fig. 4d–f). Tumour metastases consist of several distinct steps. 4T1/luc cells circulating in the peripheral blood of these mice were significantly reduced by GEP100 shRNAs (Supplementary Fig. 5). Therefore, it is very likely that the intravasation of tumour cells into blood vessels is substantially blocked by the GEP100 knockdown, as expected from our *in vitro* results.

In conclusion, our study provides a clear interpretation at a molecular level as to how EGFR expression and its signalling can be linked to the invasiveness of some breast cancer cells and to their metastatic activities. Our results also suggest that co-expression of GEP100 and EGFR may be indicative of the malignant phenotypes of primary human breast cancer. As a possible mechanism for the progression of malignancy, it is now well accepted that EGF, produced by macrophages within the tumour microenvironment, acts on some EGFR-positive breast cancer cells to induce their invasion and intravasation, that is, the early steps of metastasis[26]. Because binding of the GEP100

PH domain to tyrosine-phosphorylated EGFR is necessary to induce Arf6 activation, interfaces involved in this binding might provide excellent molecular targets for drug development of cancer therapeutics. Moreover, NIH3T3-conditioned medium contains HGF[27]. HGF receptor exhibits a close similarity to EGFR in signalling modules[8], and its overexpression also correlates well with the malignancy of mammary tumours[8]. Furthermore, Arf6/AMAP1 signalling is also used in the invasion of glioblastomas and lung tumours[9]. It will hence be interesting to investigate what other types of growth factor receptor apart from EGFR can interact with GEP100, and what other types of tumour apart from breast tumours use the GEP100/Arf6 pathway to evoke their invasiveness and to progress towards their malignancy. □

METHODS

Cells. MDA-MB-231, MCF7, Hs578T and MDA-MB-435s cells, obtained from the American Type Culture Collection, were cultured as described previously[3]. MDA-MB-231, MCF7 and MDA-MB-435s are derived from mammary-gland ductal carcinoma, and Hs578T from mammary-gland carcinoma. 4T1/luc cells expressing firefly luciferase, a gift from T. Yoneda, were cultured as described previously[3]. Fetal calf serum was purchased from Hyclone.

Antibodies and chemicals. Mouse polyclonal antibodies against ArfGEFs were generated by using GST-fusion peptides of each ArfGEF, in which the amino-acid sequences used were GEP100 (amino acids 139–248), Cytohesin-1 (5–88), ARNO (4–87), Cytohesin-3 (10–98), Cytohesin-4 (5–93), EFA6B (463–569), EFA6D (2–87), BIG2 (121–221) and KIAA0522 (479–581). Rabbit polyclonal antibodies against GEP100 were also generated accordingly. Other antibodies were purchased from commercial sources: rabbit polyclonal antibodies against haemagglutinin-tag (HA-tag) (BD Biosciences) and myc-tag (Covance); rabbit polyclonal antibodies against EGFR phosphorylated at Tyr992 (Oncogene), Tyr1045 (Cell Signaling), Tyr1086 (Abcam), Tyr1068, Tyr1148 and Tyr1173 (Biosource); and mouse monoclonal antibodies against HA-tag, myc-tag, GST-tag, EGFR and β-actin (Upstate Biotechnology), ErbB2 (Cell Signaling), GBF1 (BD Biosciences), E-cadherin (BD Transduction Lab) and Arf6 (Santa Cruz). Donkey antibodies against rabbit and mouse IgGs, conjugated with horseradish peroxidase, were from Jackson ImmunoResearch Laboratories. Alexa Fluor 647 phalloidin was from Molecular Probes. All other chemical reagents were purchased from Sigma and Wako, unless otherwise described.

Complementary DNAs. Complementary DNAs (cDNAs) encoding EFA6D, GEP100, KIAA0522 and KIAA1110 were gifts from T. Nagase (Kazusa DNA Research Institute); pGEX-PLCδ PH from M. Hirata (Kyushu University); EGFR cDNA from RIKEN BioResource Center; and GST–GGA3 from P. Randazzo (National Institute of Health). cDNAs for other ArfGEFs were amplified by using polymerase chain reaction (PCR) from first-strand cDNAs prepared from human fetal brain mRNAs (Clontech). The rescue cDNA for GEP100 was constructed by substituting the nucleotides within the siRNA target to 5′-AGGTAAAGAGCTTAGCAGAAT-3′ without changing the coding amino acids. The ΔN, ΔSec7 and ΔPH mutants of GEP100 were generated by deleting the N-terminal region (1–399), Sec7 domain (400–590) and PH domain (631–742) of GEP100, respectively. Each cDNA was ligated into pEGFP (for EGFP-tag, Invitrogen), pcDNA3 HA (for HA-tag, Invitrogen), pcDNA3 myc (for myc-tag, Invitrogen), pGEX 4T-2 (for GST-tag, Amersham Pharmacia) or pIRES (Clontech).

Transfections. cDNA transfections were performed by using Lipofectamine2000 (Invitrogen) for MDA-MB-231, MCF7 and 4T1/luc cells; and Polyfect (Qiagen) for Cos-7 cells, according to the manufacturer's instructions.

To assess Arf6-HA activities, 5×10^5 cells were co-transfected with 3 μg of pEGFP-EGFR, 0.3 μg of pcDNA Arf6-HA and 3 μg of each pcDNA myc-ArfGEF or an empty vector.

For co-precipitation assays, 5×10^5 cells were transfected with 3 μg of pEGFP-EGFR and 3 μg of each pcDNA myc-ArfGEF. After incubation for 24 h in the presence of serum, cells were starved for serum by incubating with DMEM plus 0.5% BSA for 12 h, and then stimulated with or without EGF before analyses.

For cDNA expression in MCF7 cells, 1×10^6 cells were transfected with 3 μg of pIRES plasmids, encoding EGFP/IRES/Arf6-HA, EGFP-GEP100/IRES/Arf6-HA, EGFP-GEP100(ΔSec7)/IRES/Arf6-HA, EGFP-GEP100(ΔPH)/IRES/Arf6-HA, EGFP-ARNO/IRES/Arf6-HA or EGFP-GEP100 alone. After selection by G418 (0.7 mg ml^{-1}) for 1 week, cells brightly positive for EGFP were sorted by using a fluorescence-activated cell sorter (FACSAria, Becton Dickinson). This step was repeated once again before subjecting to analyses.

For shRNA-mediated GEP100 suppression in 4T1/luc cells, 1×10^6 cells were transfected with the pSuperPuro plasmids, encoding shRNA target sequences of GEP100 or an irrelevant sequence, and cultured with 1 μg ml^{-1} puromycin for 10 days. Pools of selected cells were then subjected to analyses.

Matrigel invasion. Matrigel chemoinvasion assay was performed with Biocoat Matrigel chambers (BD Biosciences) by using NIH3T3-conditioned medium or EGF (10 ng ml^{-1}, Sigma), as described previously[3], in which 1×10^5 cells were seeded on the upper wells. After incubation for 12 h (for MDA-MB-231 and 4T1/luc cells) or 24 h (for MCF7 cells), cells were fixed in 4% paraformaldehyde, and the number of cells that migrated out to the lower surface of the membranes was scored by staining with 1% crystal violet. Data were collected from three independent experiments, each done in duplicate. In this Matrigel-invasion assay, chamber filters each 6.4 mm in diameter and containing 3×10^4 pores (each with an 8 μm diameter) were used. Therefore, the total area of the pores comprised approximately 4% of the total area of the filter. These filters were completely covered with Matrigel. Thus, even if all of the tumour cells initially loaded onto the upper chamber were highly invasive, only a small percentage of them would successfully transmigrate through the barrier of the Matrigel and through pores of the filter into the lower side of the filter, within the limited time of incubation used.

GST–GGA pulldown, immunoprecipitation and immunoblotting. Arf6 activities were measured by using GST–GGA, as previously described[13], with 300 μg of cell lysates in each assay.

For co-precipitation assays of GEP100 with EGFR, cells were lysed in RIPA buffer (1% Nonidet P-40, 1% deoxycholate, 0.1% SDS, 20 mM Tris-HCl (pH 7.4), 150 mM NaCl, 5 mM EDTA, 1 mM Na_3VO_4, 1 mM phenylmethylsulfonyl fluoride, 5 μg ml^{-1} aprotinin, 2 μg ml^{-1} leupeptin and 3 μg ml^{-1} pepstatin A). Cell lysates (300 μg) were then incubated with an anti-GEP100 polyclonal antibody or an anti-myc antibody (for myc-GEP100), coupled to Protein A-Sepharose beads.

For *in vitro* protein binding assays, 25 μg each of GST-fused PH domains of GEP100 (631–742), ARNO (261–387) or PLCδ (16–128), expressed in bacteria and purified on glutathione-beads, and 1 mg of cell lysates prepared in RIPA buffer were used.

Immunoblotting analysis, coupled with SDS–PAGE, was performed as described previously[3].

Immunofluorescent microscopy. Immunofluorescence staining of cells and acquisition of confocal images were done by using a confocal laser scanning microscope (Carl Zeiss LSM510), as previously described[3].

Immunohistochemical staining. Immunohistochemistry was performed on 4-μm-thick formalin-fixed paraffin-embedded sequential sections. All samples were reviewed independently by two pathologists to determine the histological classification of samples according to the Van Nuys classification, in which grade 1 cases correspond to noncomedo DCIS[28]. Immunohistochemical staining of GEP100 or EGFR was performed by using the standard avidin-biotin-peroxidase complex (ABC) method, as previously described[4,29]. Briefly, sections were deparaffinized in xylene and dehydrated in a graded series of ethanol, and processed for antigen retrieval by heating in 10 mM sodium citrate (pH 6.0) at 121 °C for 5 min in a pressure cooker. Endogenous peroxidase activity was blocked by 0.3% H_2O_2 in methyl alcohol at room temperature for 30 min. After rinsing in PBS and blocking with 1% goat serum (for GEP100 staining) or 1% horse serum (for EGFR staining) in PBS at room temperature for 30 min, the sections were incubated with an affinity-purified GEP100 rabbit polyclonal antibody or an anti-EGFR mouse monoclonal antibody (Novocastra) in PBS overnight at 4 °C. After rinsing in PBS, the sections were incubated with a biotinylated goat anti-rabbit IgG antibody or a biotinylated horse anti-mouse IgG antibody (Vector Lab) for 40 min and then with peroxidase-conjugated streptavidin (Vector Lab) at room temperature for 50 min. After rinsing in PBS, the colouring reaction was performed with

0.3 mg ml^{-1} diaminobenzidine and 0.003% H_2O_2 in 0.05 M Tris-HCl (pH 7.6). Each section was counterstained with haematoxylin. *P* values were calculated by using the χ^2 test.

Metastasis. Metastasis assays using 4T1/luc cells were performed as described previously[4]. Briefly, female Balb/c mice (6–8 weeks old, SLC, Japan) were anaesthetized with pentobarbital (0.05 mg g^{-1} body weight), a 2-mm skin incision was made in the right inguinal mammary fat pad and 1×10^6 4T1/luc cells in 0.1 ml PBS were injected into the tissue through a 27-gauge needle. Nineteen days later, under deep anaesthesia with ether, the left lungs and primary tumours at the originally injected fat pads were surgically removed. After taking photographs to observe the numbers and sizes of metastatic nodules on their surface, these lungs were homogenized and determined for luciferase activity by using a luciferase assay system (Promega). The primary tumours were weighed individually. The protocols used for all animal experiments in this study were approved by the Animal Research Committee of Osaka Bioscience Institute.

Accession numbers. Human GEP100, AB018306; human Cytohesin-1, M85169; human ARNO, X99753; human Cytohesin-3, NM_004227; human Cytohesin-4, NM_013385; human EFA6A, NM_002779; human EFA6B, NM_012455; human EFA6C, AL136559; human EFA6D, AB023159; human BIG1, AF111162; human BIG2, AF084521; human GBF1, NM_004193; KIAA0522, AB011094; KIAA1110, AB029033; human Arf6, NM_001663; and human EGFR, NM_005228.

Other methods. RT–PCR, siRNA, viability, matrix degradation, haptotactic migration, cell adhesion and gelatin zymography are described in Supplementary Information.

Note: Supplementary Information is available on the Nature Cell Biology website.

ACKNOWLEDGEMENTS

We thank M. Hiraishi, M. Iwahara and M. Miyoshi for their help, T. Yoneda for 4T1/luc cells, RIKEN BioResource Center, M. Hirata and P. Randazzo for cDNAs, and H. A. Popiel for reading the manuscript. This work was supported in part by grants-in-aid from the Ministry of Education, Science, Sports and Culture of Japan, and by the Mochida Memorial Foundation and the Naito Foundation.

Published online at http://www.nature.com/naturecellbiology/
Reprints and permissions information is available online at http://npg.nature.com/reprintsandpermissions/

1. Blume-Jensen, P. & Hunter, T. Oncogenic kinase signalling. *Nature* **411,** 355–365 (2001).
2. Hynes, N. & Lane, H. ERBB receptors and cancer: the complexity of targeted inhibitors. *Nature Rev. Cancer* **5,** 341–354 (2005).
3. Hashimoto, S. *et al.* Requirement for Arf6 in breast cancer invasive activities. *Proc. Natl Acad. Sci. USA* **101,** 6647–6652 (2004).
4. Onodera, Y. *et al.* Expression of AMAP1, an ArfGAP, provides novel targets to inhibit breast cancer invasive activities. *EMBO J.* **24,** 963–973 (2005).
5. Sabe, H. Requirement for Arf6 in cell adhesion, migration, and cancer cell invasion. *J. Biochem.* **134,** 485–489 (2003).
6. Sabe, H., Onodera, Y., Mazaki, Y. & Hashimoto, S. ArfGAP family proteins in cell adhesion, migration and tumor invasion. *Curr. Opin. Cell Biol.* **18,** 558–564 (2006).
7. Thompson, E. W. *et al.* Association of increased basement membrane invasiveness with absence of estrogen receptor and expression of vimentin in human breast cancer cell lines. *J. Cell Physiol.* **150,** 534–544 (1992).
8. Birchmeier, C., Birchmeier, W., Gherardi, E. & Vande Woude, G. F. Met, metastasis, motility and more. *Nature Rev. Mol. Cell Biol.* **4,** 915–925 (2003).
9. Hashimoto, S. *et al.* Targeting AMAP1 and cortactin binding bearing an atypical src homology 3/proline interface for prevention of breast cancer invasion and metastasis. *Proc. Natl Acad. Sci. USA* **103,** 7036–7041 (2006).
10. Cox, R., Mason-Gamer, R. J., Jackson, C. L. & Segev, N. Phylogenetic analysis of Sec7-domain-containing Arf nucleotide exchangers. *Mol. Biol. Cell* **15,** 1487–1505 (2004).
11. D'Souza-Schorey, C. & Chavrier, P. ARF proteins: roles in membrane traffic and beyond. *Nature Rev. Mol. Cell. Biol.* **7,** 347–358 (2006).
12. Someya, A. *et al.* ARF-GEP(100), a guanine nucleotide-exchange protein for ADP-ribosylation factor 6. *Proc. Natl Acad. Sci. USA* **98,** 2413–2418 (2001).
13. Santy, L. C. & Casanova, J. E. Activation of ARF6 by ARNO stimulates epithelial cell migration through downstream activation of both Rac1 and phospholipase D. *J. Cell Biol.* **154,** 599–610 (2001).
14. Derrien, V. *et al.* A conserved C-terminal domain of EFA6-family ARF6-guanine nucleotide exchange factors induces lengthening of microvilli-like membrane protrusions. *J. Cell Sci.* **115,** 2867–2879 (2002).
15. Price, J. T., Tiganis, T., Agarwal, A., Djakiew, D. & Thompson, E. W. Epidermal growth factor promotes MDA-MB-231 breast cancer cell migration through a phosphatidylinositol 3′-kinase and phospholipase C-dependent mechanism. *Cancer Res.* **59,** 5475–5478 (1999).
16. Honda, A. *et al.* Phosphatidylinositol 4-phosphate 5-kinase α is a downstream effector of the small G protein ARF6 in membrane ruffle formation. *Cell* **99,** 521–532 (1999).
17. Zajchowski, D. *et al.* Expression of growth factors and oncogenes in normal and tumor-derived human mammary epithelial cells. *Cancer Res.* **48,** 7041–7047 (1988).
18. Yamaji, R. *et al.* Identification and localization of two brefeldin A-inhibited guanine nucleotide-exchange proteins for ADP-ribosylation factors in a macromolecular complex. *Proc. Natl Acad. Sci. USA* **97,** 2567–2572 (2000).
19. Di Paolo, G. & De Camilli, P. Phosphoinositides in cell regulation and membrane dynamics. *Nature* **443,** 651–657 (2006).
20. Lemmon, M. A. & Ferguson, K. M. Signal-dependent membrane targeting by pleckstrin homology (PH) domains. *Biochem. J.* **350,** 1–18 (2000).
21. Bowden, E. T., Barth, M., Thomas, D., Glazer, R. I. & Mueller, S. C. An invasion-related complex of cortactin, paxillin and PKCμ associates with invadopodia at sites of extracellular matrix degradation. *Oncogene* **18,** 4440–4449 (1999).
22. Zajchowski, D. A. *et al.* Identification of gene expression profiles that predict the aggressive behavior of breast cancer cells. *Cancer Res.* **61,** 5168–5178 (2001).
23. Fitzpatrick, S. L., LaChance, M. P. & Schultz, G. S. Characterization of epidermal growth factor receptor and action on human breast cancer cells in culture. *Cancer Res.* **44,** 3442–3447 (1984).
24. Takeichi, M. Cadherin cell adhesion receptors as a morphogenetic regulator. *Science* **251,** 1451–1455 (1991).
25. Frixen, U. H. *et al.* E-cadherin-mediated cell–cell adhesion prevents invasiveness of human carcinoma cells. *J. Cell Biol.* **113,** 173–185 (1991).
26. Condeelis, J. & Pollard, J. W. Macrophages: obligate partners for tumor cell migration, invasion, and metastasis. *Cell* **124,** 263–266 (2006).
27. Rong, S. *et al.* Tumorigenicity of the met proto-oncogene and the gene for hepatocyte growth factor. *Mol. Cell. Biol.* **12,** 5152–5158 (1992).
28. Silverstein, M. J. *et al.* Prognostic classification of breast ductal carcinoma-in-situ. *Lancet* **345,** 1154–1157 (1995).
29. Toda, Y. *et al.* Application of tyramide signal amplification system to immunohistochemistry: a potent method to localize antigens that are not detectable by ordinary method. *Pathol. Int.* **49,** 479–483 (1999).

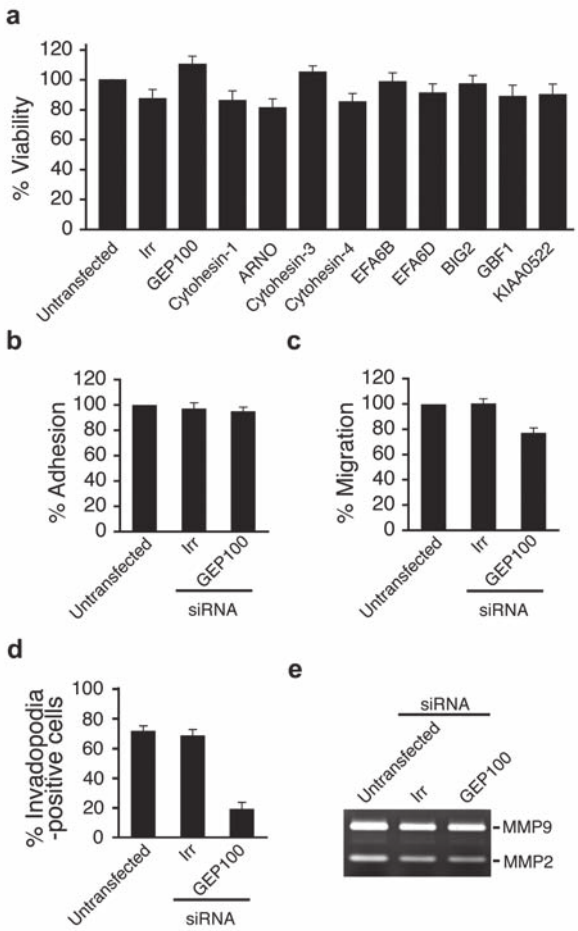

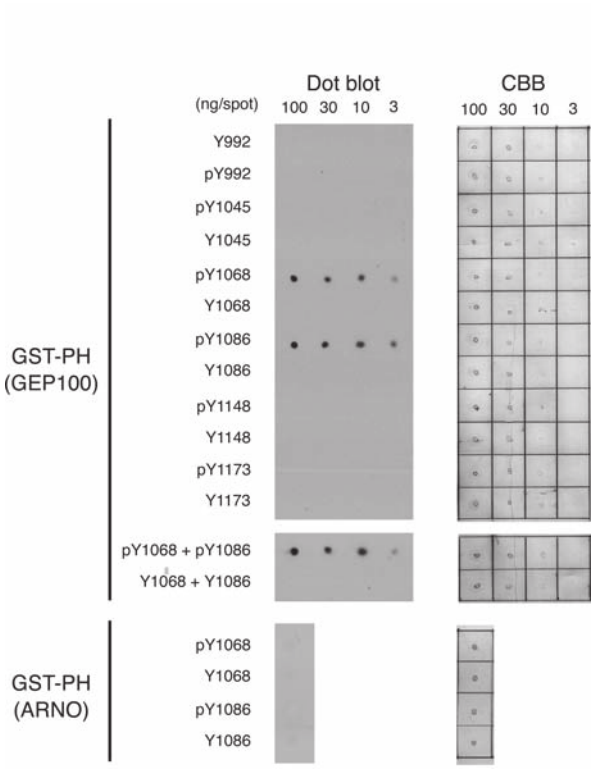

Figure S1 (a) Effects of knockdown of various ArfGEFs on cell viability in MDA-MB-231 cells. Viability of cells, used for experiments described in Figure 1b, was measured using the MTS assay. Data are presented as percentages calculated by normalizing the values obtained for the untreated cells as 100%. Error bars show mean +/- s.e.m., *n*=3, in which more than 10,000 cells were counted in each experiment. (**b-e**) Effects of GEP100 knockdown in MDA-MB-231 cells. Activities of adhesion to collagen 1 h after plating (**b**), and transmigration toward collagen in a modified Boyden chamber (*i.e.*, haptotactic migration assay without matrix degradation, **c**), and invadopodia formation (**d**). In **b** and **c**, data are presented as percentages calculated by normalizing the values obtained for the untreated cells as 100%. In **d**, data are presented as percentages of cells positive for invadopodia formation. Error bars show mean +/- s.e.m., *n*=3 (**b-d**). 5240 +/- 227 untransfected cells were calculated to have transmigrated per φ6.5 mm modified Boyden chamber filter under these conditions (**c**). Secretion of MMP2 and MMP9 were assayed in siRNA-treated cells, using the gelatin zymography method (**e**).

Figure S2 Interaction of the PH domain of GEP100, but not ARNO, with pY1068 and pY1086 peptides in a dot-blot assay. Peptides were spotted onto a nitrocellulose membrane (100, 30, 10, and 3 ng spot^{-1}), and incubated with 5 μg ml^{-1} of GST-PH proteins derived from GEP100 or ARNO after the membrane was blocked with 5% bovine serum albumin. After washing, GST proteins retained on the membranes were visualized using an anti-GST antibody (left panel). Coomassie brilliant blue (CBB) staining of the membrane is also shown in the right panel. These assays were performed at least two times and representative figures are shown.

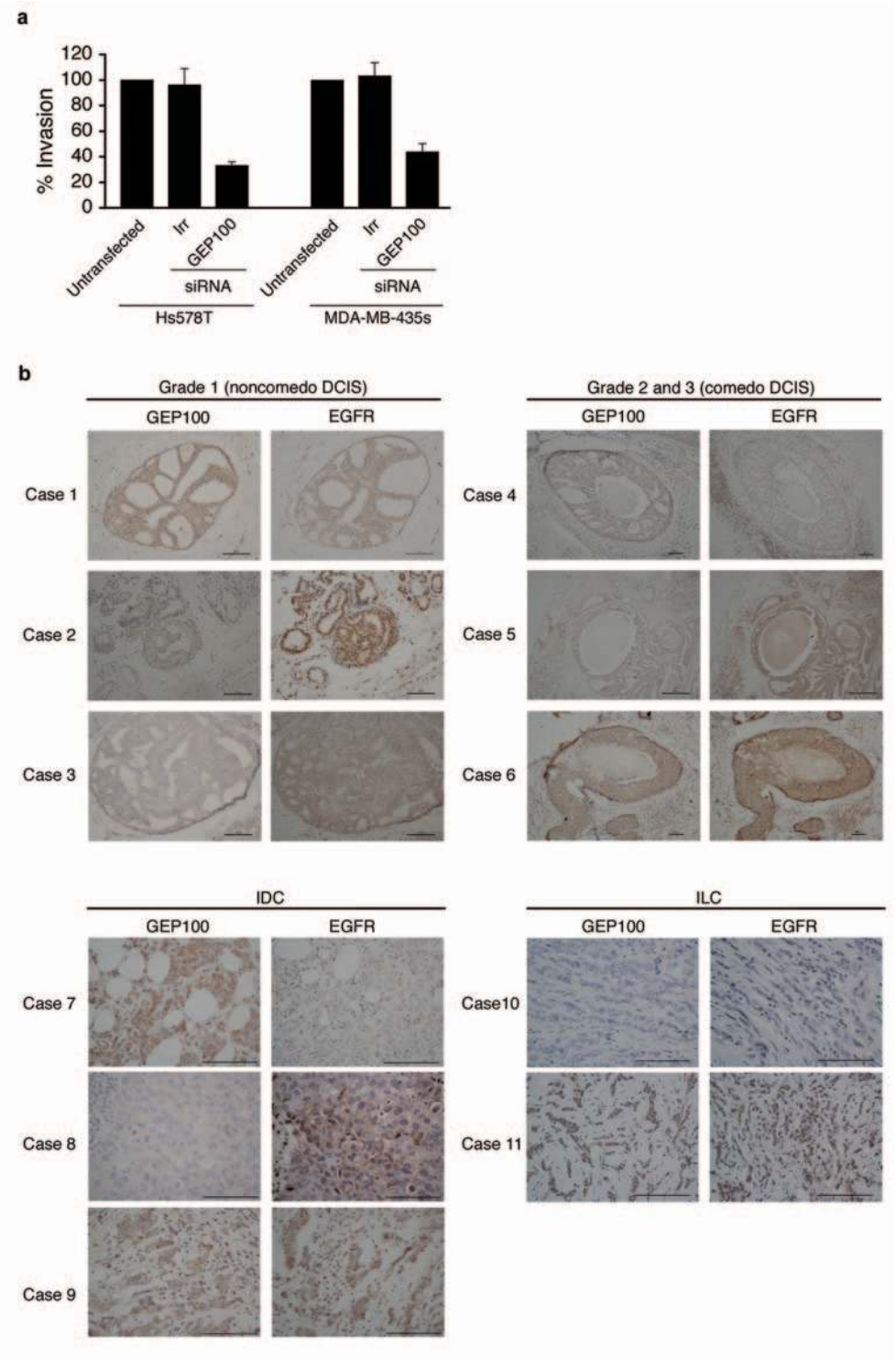

Figure S3 (**a**) Effects of GEP100 knockdown on Matrigel invasion activity in Hs578T and MDA-MB-435s cells. Data are presented as percentages calculated by normalizing the values obtained for the untreated cells as 100%. Error bars show mean +/- s.e.m., *n*=3. 2688 +/- 392 and 1410 +/- 171 untreated Hs578T (*i.e.*, about 2.7% of the initially loaded cells) and MDA-MB-435s cells (*i.e.*, about 1.4% of the initially loaded cells), respectively, were calculated to have transmigrated per φ6.4 mm Matrigel-coated Boyden chamber filter under these conditions. (**b**) Immunohistochemistry of GEP100 and EGFR in cancerous breast tissue specimens. GEP100 and EGFR were each stained in brown in sequential sections in grade 1 (Case 1-3) and grade 2 and 3 (Case 4-6) ductal carcinomas *in situ* (DCIS), invasive ductal carcinoma (IDC, Case 7-9), and invasive lobular carcinoma (ILC, Case 10 and 11). Case 1, 4 and 7, GEP100 positive and EGFR negative; Case 2, 5 and 8, GEP100 negative and EGFR positive; Case 3 and 10, double negative; and Case 6, 9 and 11, double positive. All sections were counterstained with hematoxylin, and representative figures are shown. Scale bars, 100 μm.

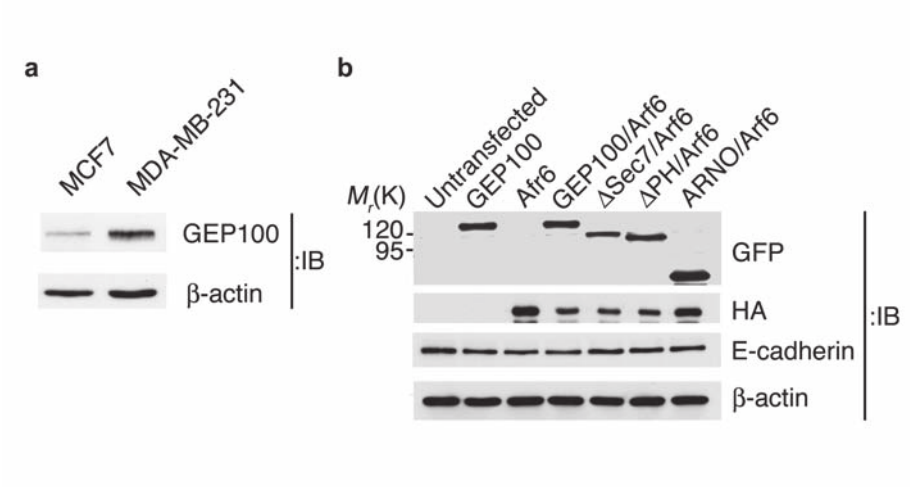

Figure S4 (**a**) Protein expression level of endogenous GEP100 in MCF7 and MDA-MB-231 cells, as assessed by anti-GEP100 immunoblot. The β-actin blot is included as a control. Ten μg of cell lysates were used. (**b**) Protein expression in MCF7 cell lysates (10 μg), used in experiments shown in Figure 3a, was analysed by immunoblots as indicated. The β-actin blot is included as a control.

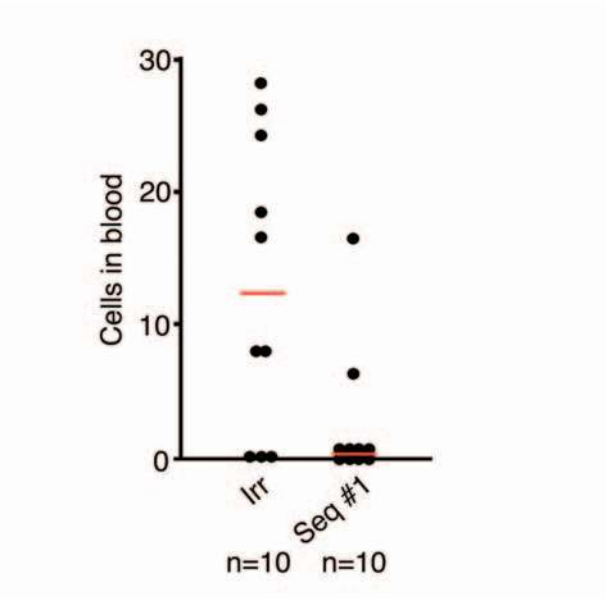

Figure S5 GEP100 knockdown blocks intravasation of 4T1/luc cells into blood vessels. 4T1/luc cells, transfected with GEP100 Seq #1 plasmid (Seq #1) or with a plasmid with an irrelevant sequence (Irr), were injected into fat pads and the number of circulating cells were quantified 19 days later. Median values are shown as red lines. *n*=10 for each case.

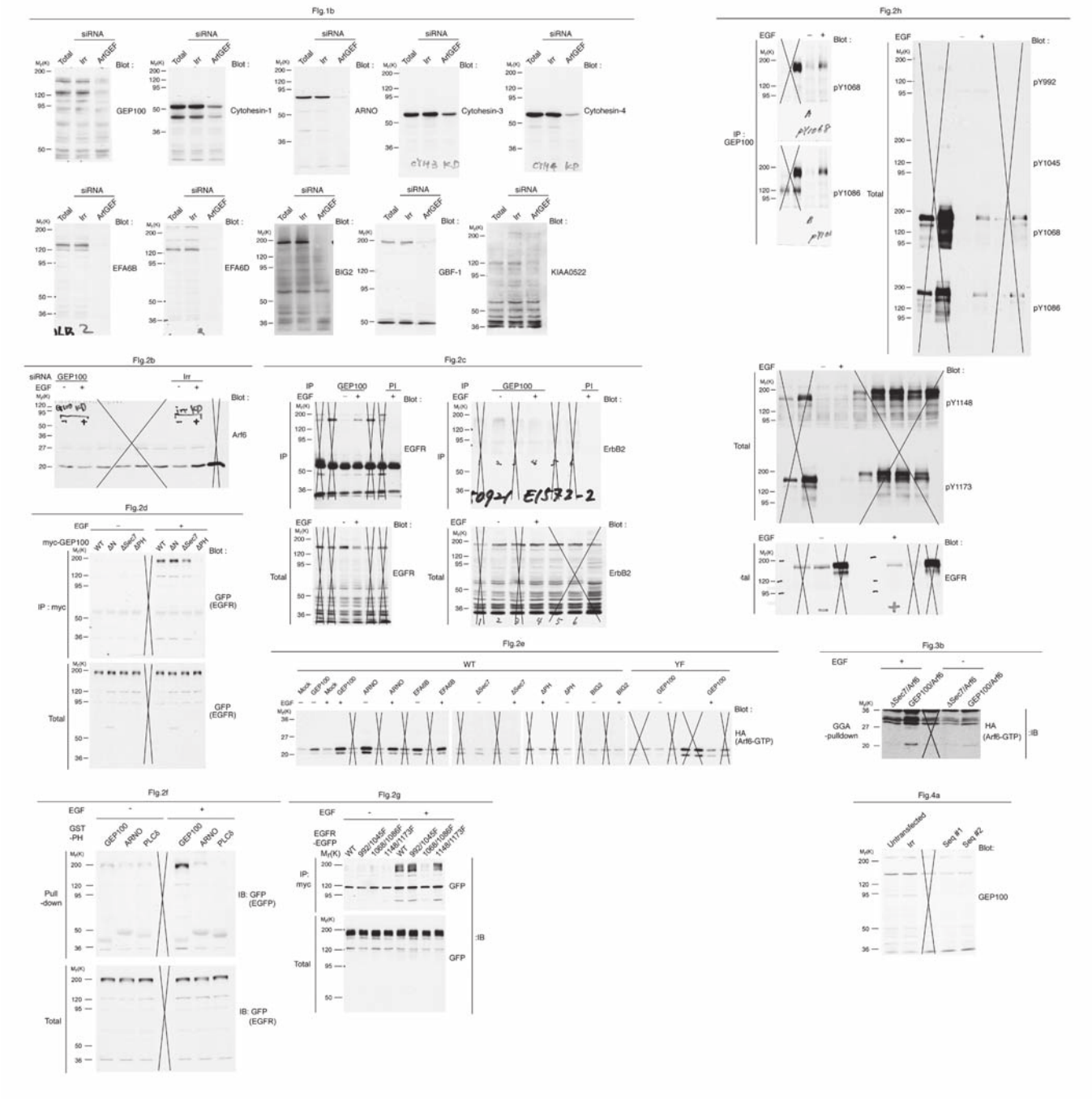

Figure S6 Uncropped images of blots shown in Fig. 1b, 2b-h, 3b and 4a. Sections irrelevant for the images shown in the respective figures are crossed out.

Supplementary Information

Methods

RT-PCR. Total RNA was extracted from cultured cells using Qiagen RNeasy Mini Kit, and reverse-transcribed by M-MLV Reverse Transcriptase (Promega) using oligo dT primers at 42 ^{o}C for 60 min. cDNAs were then subjected to 35 cycles of PCR amplification, each cycle consisting of 95 ^{o}C for 2 min, 95 ^{o}C for 30 sec, 50 ^{o}C (for *BIG1*), 51 ^{o}C (for *EFA6D* and *Cytohesin-3*), 53 ^{o}C (for *GEP100*, *Cytohesin-1*, *Cytohesin-4*, *EFA6B* and *GBF1*) or 57 ^{o}C (for *ARNO*, *EFA6A*, *EFA6C*, *BIG2*, *KIAA0522* and *KIAA1110*) for 30 sec, and 72 ^{o}C for 30 sec. The primers used were: for *GEP100*, 5'-GCCTTTAGCAACGATGTCATC-3' and 5'-CACATGGTCCTCATTGGTCTT-3'; for *Cytohesin-1*, 5'-TAGCTAATGAAATTGAAAACCTGGGAT-3' and 5'-TTCATGGCAATGAACCTCTCCACAGTG-3'; for *ARNO*, 5'-CAGTGAAGCCATGAGCGAGGT-3' and 5'-TTCATGGCCACAAAGCGCTCCAGG-3'; for *Cytohesin-3*, 5'-ATCGACAATCTAACTTCCGTA-3' and 5'-ATGGCGATGAACCGTTCTGCCGTG-3'; for *Cytohesin-4*, 5'-TGTTTGCCCAAATCGACTGCT-3' and 5'-TCATCCACCTTCTGCACCGAG-3'; for *EFA6A*, 5'-AGCCAGCTGGTGTCCGACTCA-3' and 5'-GGAGCTAACAGCAGCTGGGAA-3'; for *EFA6B*, 5'-GAGGACACCGATGAACTCTTC-3' and 5'-GTGTCTTCTTCATCCACGG-3'; for *EFA6C*, 5'-GGATGGCCTGTCAGACTCAGA-3' and 5'-CCTCAGCTCATCCTCATCAATGG-3'; for *EFA6D*, 5'-CAACACGGCTAGAAGCTCATT-3' and 5'-TTCATCATCTACTGCCCATTC-3'; for *BIG1*, 5'-ACAGATACGGAAGTTTAAATT-3' and 5'-

TTATACAGAAGTCTTCTTTGT-3'; for *BIG2*, 5'-CATGGCAAGACGGTGTAGTGT-3' and 5'-CTCTAAGTTGTACAGCAGCCGCCGC-3'; for *GBF1*, 5'-GAAGGCACAGCTTTGGTC-3' and 5'-GCTTGGTCTGGCTGTCTCCTT-3'; for *KIAA0522*, 5'-AAGTGCGAGGCAGCAGGCGAG-3' and 5'-ATCGTTGGTCCGCAGTTCACG-3'; for *KIAA1110*, 5'-ACGCTCTCCACCGACACCCTG-3' and 5'-ACCTTGGTGACGTACGTGACG-3'.

siRNA. Cells cultured in growth medium were transfected with 50 nM of oligonucleotide duplexes using Oligofectamine (Invitrogen) and incubated for 48 h before being subjected to analyses. Nucleotide sequences used were: for *GEP100* 5'-AAGTGAAATCACTGGCCGAGT-3'; for *Cytohesin-1*, 5'-AACGACCTCCTGAAGAACACT-3'; for *ARNO*, 5'-AAGATGGCAATGGGCAGGAAG-3'; for *Cytohesin-3*, 5'-AAAACGACTCAGAGGAACAAA-3'; for *Cytohesin-4*, 5'-AAGAGTGAGCCATTCTCCATC-3'; for *EFA6B*, 5'-AATGAAGACTCAGGGGAAGAC-3'; for *EFA6D*, 5'-AAGGAGACCCCAGAAAATCTC-3'; for *BIG2*, 5'-AAGCGGCTGATCGACAGAATT-3'; for *GBF1*, AATCCACACGACCGCCATAAC; for *KIAA0522*, 5'-AAGTGCGAGGCAGCAGGCG-3'. An siRNA duplex with an irrelevant sequence (5'-GCGCGCUUUGUAGGAUUCG-3' and 5'-CGCGCGAAACAUCCUAAGC-3') was purchased from Dharmacon.

For silencing of *GEP100* in mouse 4T1/luc cells, the *GEP100*-shRNA-targeting sequences used were 5'-AGGTGAAATCCCTGGCTGAAT-3' (sequence #1) and 5'-AAGCGCTCTCGGTCACTCTCC-3' (sequence #2). The insert for *GEP100*-shRNA

sequence #1, or sequence #2, or an irrelevant sequence, which is the same as that used for the irrelevant siRNA, was subcloned into pSuperPuro vector (OligoEngine), according to the manufacturer's instructions.

Viability. Cell viabilities were measured using a 3-(4,5-dimethylthiazol-2-yl)-5-(3-carboxyphenyl)-2-(4-sulfophenyl)-2H-tetrazolium (MTS) colorimetric assay kit (Promega), according to the manufacturer's instructions.

Invadopodia formation. The number of cells forming invadopodia were measured as described previously[1,2,3]. Briefly, porcine skin gelatin (Type A with 300 Bloom, Sigma) was conjugated with Alexa Fluor 594 (Molecular Probes), and glass-bottomed dishes (MatTek) were coated with the gelatin and subsequently cross-linked with 0.5% glutaraldehyde. Cells in growth medium were then replated onto these dishes and incubated for 16 h, then fixed in 4% paraformaldehyde for 10 min at room temperature. Cells were then labelled with an anti-cortactin antibody and phalloidin. Cells with gelatin degradation areas ($\geq$1 μm in diameter), and also positive for both cortactin and F-actin at sites of the gelatin degradation, were scored as positive for invadopodia formation[3]. Data were collected from three independent experiments, each done in duplicate, in which more than 100 cells were analyzed using a confocal laser scanning microscope (LSM 510, Carl Zeiss) at a x 63 magnification.

Haptotactic migration and cell adhesion. Haptotactic cell migration assay was performed in the absence of serum using modified Boyden chambers (Transwell with 8 μm pores, Costar), in which the lower surface of the membrane was coated with collagen type I (10 μg ml^{-1}), and $0.3x10^5$ cells were seeded on the upper wells, as previously

described[1,2]. Cell adhesion onto collagen type I-coated dishes (10 μg ml^{-1}) was analysed, as described previously[1,2].

Gelatin zymography. 5 x 10^5 siRNA-transfected cells were incubated in the presence of serum for 12 h, and the cultured medium was harvested and centrifuged at 10,000 x *g* for 2 min. The supernatants were then concentrated using a Centricon centrifugal filter (10 kDalton cut size, Millipore), separated by SDS-PAGE, and subjected to zymography for gelatin degradation, as previously described[1,2].

Peptides. Peptides were synthesized by Sigma Genosys. The sequences of EGFR-derived peptides were as follows: peptide Y992 (Y992), DADEYLIPQQGF; Y1045, SFLQRYSSDPTGAL; Y1068, DTFLPVPEYINQS; Y1086, SVQNPVYHNQPLN; Y1148, DNPDYQQDF; and Y1173, ENAEYLRVA. Tyrosines in each peptide were phosphorylated for the phospho-Tyr peptides.

Intravasation assay. Circulating 4T1/luc cells were quantified as described previously[4]. Briefly, 19 days after injection of 4T1/luc cells into fat pads, similar to the metastasis assays, mice were anesthetized with pentobarbital (0.05 mg g^{-1} body weight) and 1 ml of blood was collected by heart puncture and centrifuged. The serum/buffy-coat layers were plated in 1 ml of DMEM:F12 (50:50)/10% FCS. After 24 h, the plates were washed with PBS to remove erythrocytes and fresh medium containing 1 mg ml^{-1} G418 was added to selectively grow 4T1/luc cells. After 7 days, colonies were stained with hematoxylin and counted.

References for Supplementary Methods

1. Hashimoto, S. *et al.* Requirement for Arf6 in breast cancer invasive activities. *Proc. Natl Acad. Sci. USA* **101,** 6647-6652 (2004).
2. Onodera, Y. *et al.* Expression of AMAP1, an ArfGAP, provides novel targets to inhibit breast cancer invasive activities. *EMBO J.* **24,** 963-973 (2005).
3. Buccione, R., Orth, J. D. & McNiven, M. A. Foot and mouth: podosomes, invadopodia and circular dorsal ruffles. *Nat. Rev. Mol. Cell Biol.* **5,** 647-657 (2004).
4. Wyckoff, J. B., Jones, J. G., Condeelis, J. S. & Segall, J. E. A critical step in metastasis: *in vivo* analysis of intravasation at the primary tumor. *Cancer Res.* **60,** 2504-2511 (2000).